CryoLetters 45(2), 69 – 87 (2024)

https://doi.org/10.54680/fr24210110112

PERSPECTIVE

TARGETED DEVELOPMENT AND OPTIMIZATION OF SMALL-MOLECULE ICE RECRYSTALLIZATION INHIBITORS (IRIs) FOR THE CRYOPRESERVATION OF BIOLOGICAL SYSTEMS

Leah E. McMunn [1ǂ], Ellyssa M. Walsh [1ǂ] and Robert N. Ben [1*]

[1] Department of Chemistry and Biomolecular Sciences, University of Ottawa, Ottawa, ON, Canada
ǂ Indicates equal contribution.
* Corresponding author's E-mail: robert.ben@uottawa.ca

Abstract

Despite the routine use of cryopreservation for the storage of biological materials, its outcomes are often sub-optimal (including reduced post-thaw viability, recovery, and functionality) due to the damage caused by uncontrolled ice growth. Traditional cryoprotective agents (CPAs), including dimethyl sulfoxide (DMSO), fail to prevent damage caused by ice growth and concerns over CPA cytotoxicity have fostered an increased interest in developing improved CPAs and cryoprotection strategies. The inhibition of ice recrystallization by natural antifreeze (glyco)proteins [AF(G)Ps] to improve cryopreservation outcomes has been examined; however, the ice binding properties of these substances and their challenging large-scale production make them poor CPA candidates. Therefore, the development and deployment of biocompatible, small-molecule ice recrystallization inhibitors (IRIs) for use as CPAs is a worthwhile objective. Extensive structure-activity relationship studies on AF(G)Ps revealed that simple carbohydrate derivatives could inhibit ice recrystallization. It was later discovered that this activity could be fine-tuned by delicately balancing the molecule's hydrophobicity and hydrophilicity. Current generation small-molecule IRIs have been meticulously designed to avoid binding to the surface of ice and subsequent biological testing (for both cytotoxicity and cryopreservation efficacy) has demonstrated significant improvements to the cryopreservation outcomes of several cell types. However, an individualized cell-specific approach for the simultaneous assessment of multiple cryopreservation outcomes is necessary to realize the full potential of IRIs as CPAs. This article provides a detailed overview of the development of small-molecule carbohydrate-based IRIs and highlights the crucial cell-specific biological considerations that must be taken into account when assessing cryopreservation outcomes.

Keywords: cryopreservation; cryoprotective agent; ice recrystallization inhibition; small-molecule.

INTRODUCTION

The development and distribution of biological materials for use as medical therapeutics critically relies on successful biopreservation methods (1, 2, 3, 4). Cryopreservation at low sub-zero temperatures (< -80 °C) plays a key role by dramatically

extending the shelf-life of cellular products by slowing/stopping all biological processes. However, ice formation and growth that occurs during cryopreservation causes cells to endure significant physical and chemical stress (5, 6, 7, 8). These stressors, if not adequately mitigated, lead to cellular injury (cryoinjury) that reduces the recovery and viability of cryopreserved products (9). More importantly, cryoinjury can result in reduced functionality and efficacy of a biotherapeutic for clinical applications (3, 10, 11).

There are many factors that must be considered when attempting to minimize cryoinjury and achieve optimal cryopreservation outcomes. However, with a fundamental understanding of cryopreservation and careful control of crucial parameters (2, 4, 5, 6, 11, 12, 13, 14), the earliest examples of cryopreservation were reported in the 1940s (14, 15, 16, 17, 18, 19). More recently, the successful cryopreservation of stem cell products has revolutionized the regenerative medicine field (14, 20, 21). For example, hematopoietic stem cells (HSCs) are a life-saving treatment for dozens of conditions and these cells are routinely cryopreserved as an integral part of the world-wide transplantation supply chain (3, 14, 22, 23, 24).

To mitigate cryoinjury induced cell death in a typical cryopreservation procedure, cell media is formulated with a cryoprotective agent (CPA) prior to freezing (13). Dimethyl sulfoxide (DMSO), which was first reported as a CPA in 1959 (25), is the most widely used CPA to date, and is regarded as the gold-standard for cryopreservation (4, 13). While the use of DMSO aims to increase the number of viable cells after freezing, DMSO also exhibits toxicity and undesired side effects that are problematic for its use in clinical cryopreservation applications (26, 27, 28, 29, 30). As a result, a reduction in total DMSO concentration by the addition of various sugars (mono- and di-saccharides) or polymers (31, 32), as well as DMSO-free CPAs have been examined (26). However, these approaches continue to suffer from sub-optimal cryopreservation outcomes (reduced viability, recovery, and/or functionality). Therefore, despite the use of cryopreservation for many cell types that are highly relevant for research and clinical applications, there exists an urgent need for improvement. Furthermore, currently used CPA formulations fail to address the impact of ice recrystallization on cryopreservation outcomes (40, 41).

Ice recrystallization, which is defined as the growth of larger ice crystals at the expense of smaller crystals, causes significant cell damage and death if not controlled during cryopreservation (4, 7, 8, 9). Thus, the development of compounds that can inhibit ice recrystallization (known as ice recrystallization inhibitors, IRIs) that can be used in CPA formulations is imperative to further improving cryopreservation outcomes.

The ability to inhibit ice recrystallization was first discovered in a classification of naturally occurring peptides and glycopeptides known as biological antifreezes (BAs). These antifreeze proteins (AFPs) and glycoproteins (AFGPs) were first discovered in Antarctic fish in the 1950s and were later reported in other animals, insects, and fish that inhabit sub-zero temperature environments (42, 43, 44, 45, 46). In addition to inhibiting ice recrystallization, BAs can bind to the ice crystal surface, resulting in thermal hysteresis (TH), a phenomenon that selectively depresses the freezing point of a liquid relative to its melting point (47, 48, 49, 50, 51, 52, 53).

In nature, where temperatures drop only a few degrees, the presence of AF(G)Ps causes the fluids of an organism to become super-cooled, and while stochastic nucleation of ice occurs, the solution does not freeze. However, when temperatures drop below the depressed freezing point, rapid “needle-shaped” ice growth occurs as a result of ice binding (8, 54). This effect, known as dynamic ice shaping (DIS), is detrimental and/or lethal to cells and is especially problematic when considering that cryopreservation temperatures are significantly colder than the largest known BA-induced TH gap (53).

Furthermore, as mentioned earlier, large-scale *de-novo* synthesis and natural product isolation to commercially manufacture natural AF(G)Ps for the cryopreservation of biologics are not feasible due to economic and sustainability barriers, as well as the insufficient quantities of material that can be obtained (55, 56). While modern molecular biology techniques (e.g., heterologous protein expression) allow natural AF(G)Ps to be produced in greater quantities, the resulting cost remains too high for the obtained yields, ultimately restricting large-scale adoption of these methods (57, 58, 59).

Despite the barriers associated with *de-novo* synthesis, it is the only production method that permits the direct chemical modifications (atom-by-atom) necessary for rational and targeted design of bio-active molecules. Therefore, due to the interest in compounds that can selectively inhibit ice recrystallization (without the presence of TH activity or DIS), a rational design approach beginning with a fundamental understanding of the essential structural features of AF(G)Ps required for ice recrystallization inhibition activity was critical. This is the only approach that will lead to the discovery of compounds (i.e., small-molecule IRIs) that can be readily deployed on large scale, which is of immediate and significant need for biopreservation applications.

ASSAYS FOR DETERMINING ICE RECRYSTALLIZATION INHIBITION ACTIVITY

The ability to assess the ice recrystallization inhibition activity of a compound both reliably and quantitatively is essential for the development of improved CPAs. Several methods have been reported to assess this activity including the capillary method (60), the sucrose sandwich assay (SSA) (61), the gold nanoparticle assay (62), the sapphire slide assay (63), and the splat-cooling assay (SCA) (64, 65, 66, 67). Using these assays, qualitative and/or quantitative activity information about ice crystal size in the presence and absence of an IRI candidate can be obtained. The SSA and SCA are the two most used assays for quantitatively assessing ice recrystallization inhibition activity. The SSA uses an aqueous sucrose buffer (typically 40 %) and requires long annealing times (> 40 minutes) to allow for sufficient ice crystal growth prior to data analysis. To contrast, the SCA generally uses an aqueous salt buffer and short annealing times (< 30 minutes). To improve the reliability of the SCA for determining very small differences in ice recrystallization inhibition activity, a kinetic analysis of ice recrystallization using multiple annealing times (rather than a single time point measurement) is required (68, 69).

The Splat Cooling Assay (SCA)

Initially reported in 1988, the classic SCA drops a 10 μL aliquot of a target compound dissolved in a salt buffer solution onto a precooled aluminum plate (-78 °C) (64). As the droplet splats onto the surface, it freezes into an ice wafer (~ 5 mm in radius and < 50 μm thick) that can be transferred to a Peltier unit held below 0 °C to anneal (64). Annealing time and temperature can be varied to change the rate of ice recrystallization and the physical properties of the ice structure; longer annealing times and higher annealing temperatures result in larger ice crystals. Ice crystals can then be imaged using a camera-fitted microscope and analyzed to determine a compound's ability to inhibit ice recrystallization. The output of the initial SCA method affords semi-quantitative data by reporting the mean largest two-dimensional ice grain size as a function of annealing time (64). Modifications later made by Horwath et al. improved the quantitative output of the assay by approximating ice crystal shape as elliptical to calculate mean ice crystal area (65). However, this analysis method requires users to manually calculate area by hand, and therefore is time-consuming to complete (65, 66). In addition, ice crystal shape is poorly approximated by a linear dimension or elliptical area, therefore these initial methods of analysis had limitations with respect to accurately and reliably quantifying ice recrystallization inhibition activity.

In 2007, Jackman et al. developed a method for the SCA that decreases analysis time and quantifies ice recrystallization inhibition activity using domain recognition software (DRS) (66). This method uses the general experimental assay protocol described by Knight et al. (64), with an annealing temperature of -6.4 °C and annealing time of 30 minutes (66). Once ice wafer images are obtained, the DRS is used to randomly select 12 crystals from an ice wafer image for which the user could identify each crystal's boundary and calculate its complex cross-sectional area without shape-related assumptions (66). The ice recrystallization inhibition activity of a compound is then quantified as a percent mean grain size (% MGS) of the ice crystals at a designated compound concentration relative to the phosphate-buffered saline (PBS) control. The quantitative % MGS output allowed for direct comparison of ice recrystallization inhibition activity between multiple compounds within a library at the same concentration. However, significant drawbacks to this iteration of the SCA remain. Firstly, it only provides a snapshot of ice recrystallization inhibition activity and therefore fails to address the concentration- and

time-dependence of crystal growth (66, 67). Secondly, this method underestimates the heterogenous nature of ice crystals by only quantifying the area of a small, random sub-set of ice crystals (66, 67).

To address these issues, further modifications to the SCA were reported by Abraham et al. in 2015 (67). With this version of the assay, compounds are tested at multiple concentrations and annealed for multiple time points at -6.4 °C to capture a full kinetic profile of ice recrystallization inhibition activity (67). During data analysis, the cross-sectional area of all ice crystals within a field of view is determined [assisted by image processing software such as ImageJ (71)], and therefore, the heterogeneity of each ice wafer is accounted for (67). The data is then fit to a monoexponential growth model and first-order rate constants are derived that describe the increase in mean ice crystal area over time (67). With this model, short annealing times capture inhibition activity during the period with the highest rate of recrystallization, while longer annealing times approximate the "end-point" of ice crystal growth (54, 66, 67). Determining a full kinetic profile of inhibition activity remains time-consuming due to the number of data points that need to be collected. Further investigation found that the initial rate of ice recrystallization

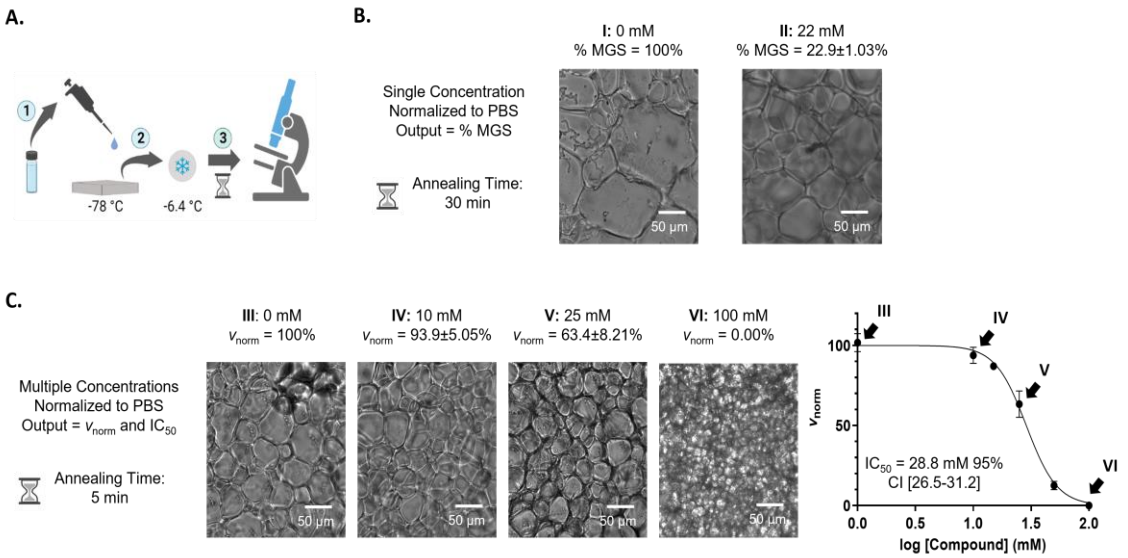

Figure 1. (A) General schematic for the splat cooling assay (64, 66, 67). **(B)** Representative data using a 30-minute annealing time at -6.4 ˚C to determine % mean grain size (% MGS) of a single compound concentration normalized to phosphate-buffered saline (PBS); n = 3, mean ± SD. **(C)** Representative data using a 5-minute annealing time at -6.4 ˚C to determine the IC_{50} from analysis of multiple compound concentrations; n = 3, mean ± SD. The initial rate (v) of ice crystal growth is calculated for each individual concentration and normalized to the rate (v) of the PBS control to give v_{norm} as a percent rate relative to PBS. Images of ice wafers at selected concentrations are distinguished by roman numeral and directly correspond to data points on the dose response curve.

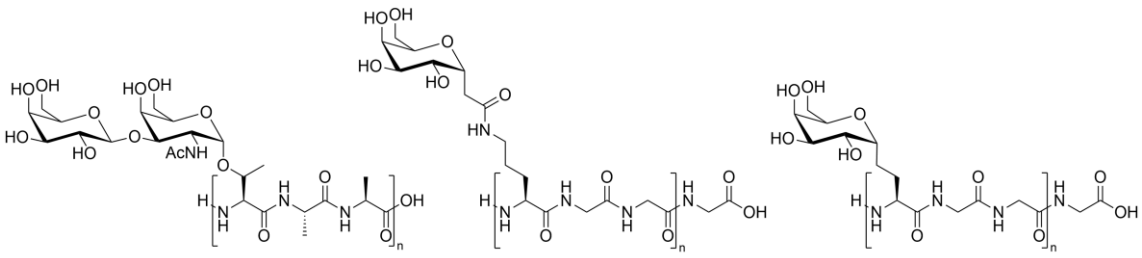

Figure 2. Structures and ice recrystallization inhibition activity of representative antifreeze glycoprotein (AFGP-8) and select *C*-linked analogues OGG-Gal and *C*-serine (84, 85).

inhibition, using a single five-minute annealing time, is in good statistical agreement with the full kinetic profile (72). With this simplified five-minute annealing SCA, the analysis of multiple compounds can be completed in a short amount of time without significantly extending the active data collection time compared to the full kinetic analysis of a single compound (72). For each compound tested, the initial rate (v) of ice crystal growth is calculated for each concentration and normalized to the rate (v) of the PBS control to give v_{norm} as a percent rate relative to PBS. By fitting the normalized initial rates of ice crystal growth at multiple concentrations to a four-parameter dose-response model, an IC_{50} for ice recrystallization inhibition activity can be calculated (67, 72). Thus, this SCA method provides information on the rate of ice recrystallization inhibition, the concentration dependence and cooperativity of an IRI, and allows for direct comparison of activity between compounds via the IC_{50} value. An overview of the two different protocols for the SCA that are commonly used to assess the activity of small-molecule IRIs is provided in Figure 1 and includes representative images of ice wafers from each assay.

Recently, developments towards automated image analysis for ice recrystallization inhibition activity analysis have been explored (73, 74, 75). However, these methods can be inaccurate when ice crystals reside in multiple focal planes and/or when the ice crystal borders are poorly defined within an image. Additional development and training of automation methods is required before they can be used for the reliable quantification of ice recrystallization inhibition activity. Therefore, visual determination of ice crystal measurements, assisted by image processing software, remains the primary method of analysis for the determination of ice recrystallization inhibition activity to date.

In the Ben laboratory, the SCA protocols developed by Jackman et al. (66) and Abraham et al. (67, 72) are both extensively used in the development process for small-molecule IRIs. The preliminary screening of candidate IRI molecules is often accomplished using a 30-minute annealing time at a single compound concentration followed by data analysis as described by Jackman et al. (66). Once a hit compound is discovered, more detailed dose-dependent activity information is then determined using the assay method described by Abraham et al. (67, 72).

DEVELOPING SMALL-MOLECULE IRIs

To rationally design effective small-molecule IRIs, it is necessary to obtain a fundamental understanding of the key structural features of AFPs and AFGPs that are required for their ice recrystallization inhibition activity. Early structure-activity relationship (SAR) studies of AF(G)Ps focused primarily on how structural modifications affected TH activity, and very few assessed the features necessary for ice recrystallization inhibition (55, 76, 77, 78, 79, 80, 81, 82, 83). In the early 2000's, a study by Ben et al. serendipitously found that ice recrystallization inhibition and TH activity could be decoupled and isolated (84, 85). These studies synthesized and evaluated several carbon-linked (*C*-linked) AF(G)P analogues, originally aiming to improve the metabolic stability of natural oxygen-linked AF(G)Ps (84, 85, 86). Two of the compounds, OGG-Gal and *C*-serine (Figure 2), are the first reported examples of synthetic AF(G)P analogues that possess only ice recrystallization inhibition activity and little-to-no TH activity and/or DIS (84, 85). Importantly, OGG-Gal (1.0-1.5 mg/mL) results in a percent post-thaw viability comparable to a 2.5 % DMSO control for the cryopreservation of human embryonic liver cells (87), indicating that TH activity is not required to improve cryopreservation outcomes. These results transformed the landscape of ice recrystallization inhibition research and formed the foundation for the further development of IRIs.

Since these reports, other compounds including biomass nanocelluloses (88) and synthetic polymers (89, 90) have been reported as active IRIs without TH activity. However, the practical adoption of large (glyco)peptides and polymers for cryopreservation is limited (80, 91). Small-molecule IRIs are more desirable as CPA target molecules given their ease of large-scale preparation and reduced risk of antigenicity. On-going studies with *C*-linked AF(G)P analogues found that modifications to their carbohydrate unit could modulate ice recrystallization inhibition activity (92). This finding led to the discovery that simple carbohydrates have measurable ice recrystallization inhibition activity (Figure 3),

where D-galactose is the most active of the monosaccharide IRI candidates tested (93). While the activity of D-galactose was considerably less than AFGP analogue OGG-Gal (93,94), the simplicity and accessibility of the monosaccharides warranted further investigation into the mechanism by which they inhibit ice recrystallization to enable further optimization.

It is well established that ice recrystallization is a thermodynamically-driven process that favours the formation of larger ice crystals via the transfer of water molecules from one crystal to another through the bulk water phase (54). This process has been extensively studied in metallurgical literature and can be described by the theories of Ostwald ripening (95, 96, 97) and grain boundary migration (98, 98, 100). Inhibition of ice recrystallization by AF(G)Ps is known to be due to ice binding, as previously discussed. However, the mechanism by which small molecules inhibit ice recrystallization is less understood. TH activity and DIS are not observed for small-molecule IRIs, therefore it has been suggested that their activity was not due to ice binding (93). Recent studies have supported this initial hypothesis using nuclear magnetic resonance relaxation measurements (101).

From these studies it is reported that small-molecule IRIs are excluded from the ice lattice during freezing and are concentrated in the interstitial liquid phase between ice crystals (101). Therefore, these compounds have a different mechanism of action for inhibiting ice recrystallization than AF(G)Ps and is thought to be due to an ability to disrupt the process of water molecule transfer between ice crystals that occurs during recrystallization (92, 93).

Studies have shown that a greater hydration number (the volume of space a molecule occupies upon hydration with water) is associated with a poor "fit" within the bulk water network (102). Thus, it was thought that a more highly hydrated monosaccharide would disrupt the bulk water network, prevent the transfer of water during recrystallization, and ultimately exhibit stronger inhibition activity. In fact, the ice recrystallization inhibition activity of simple carbohydrates can be directly correlated as expected (e.g. least hydrated D-talose is least active and most hydrated D-galactose is most active) (92, 93, 102). Based on the above, small molecules that dramatically

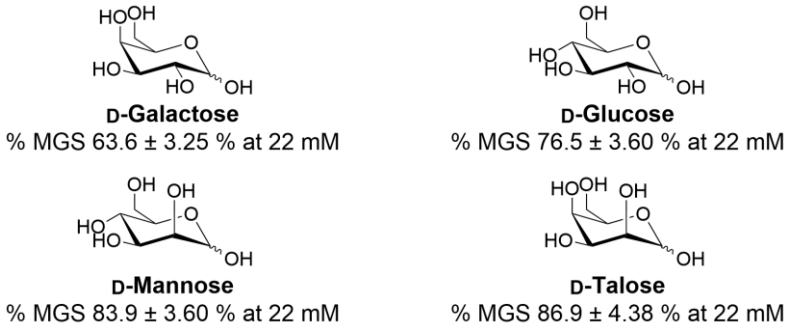

Figure 3. Structures and ice recrystallization inhibition activity of representative carbohydrate monosaccharides D-galactose, D-glucose, D-mannose, and D-talose (93).

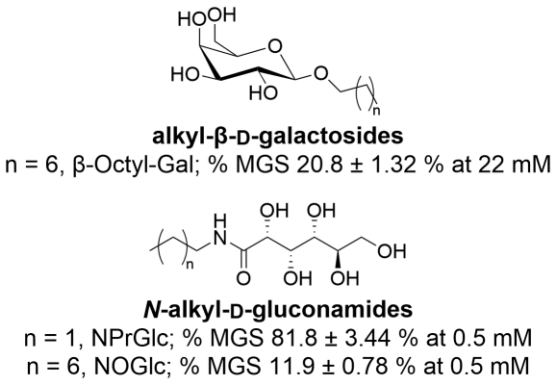

Figure 4. Structures and ice recrystallization inhibition activity of representative surfactant and hydrogelator compounds β-octyl-Gal, NPrGlc, and NOGlc (103,104).

alter and/or sequester water, such as surfactants and hydrogelators, were considered as potential IRI candidates.

These studies resulted in the identification of two classes of carbohydrate-based non-ionic surfactants and hydrogelators as active IRIs: *O*-alkyl-β-D-galactosides and *N*-alkyl-D-gluconamides (Figure 4) (103). In particular, the hydrogelator *N*-octyl-D-gluconamide (NOGlc) and the surfactant n-octyl-β-D-galactopyranoside (β-octyl-Gal) have ice recrystallization inhibition activity comparable to that of OGG-Gal and nearing the activity of native AF(G)Ps (e.g. AFGP-8) (94, 103). However, unlike native AF(G)Ps these small-molecule IRIs can be easily synthesized in less than two steps from commercially available reagents and do not exhibit TH activity or DIS (103).

Further investigation of NOGlc and β-octyl-Gal revealed that their ice recrystallization inhibition activity is not related to micelle formation or supramolecular organization despite their surfactant-like structure (103). In addition, comparison of alkyl chain length within the *N*-alkyl-D-gluconamide family of compounds suggests that a minimum threshold of hydrophobicity is required for strong inhibition of ice recrystallization (i.e., *N*-propyl-D-gluconamide, NPrGlc, has little-to-no measurable activity at 22 mM) (103, 104).

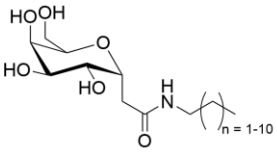

***N*-alkyl-2-(α-D-galactopyranosyl)-ethylamides**
n = 1; % MGS 67.7 ± 2.78 % at 22 mM
n = 4; % MGS 55.9 ± 3.47 % at 22 mM
n = 6; % MGS 9.0 ± 0.35 % at 22 mM

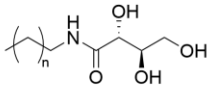

***N*-alkyl-erythronamides**
n = 4; % MGS 67.6 ± 4.64 % at 22 mM
n = 6; % MGS 56.4 ± 2.65 % at 22 mM

Figure 5. Structures and ice recrystallization inhibition activity of representative *N*-alkyl-2-(α-D-galactopyranosyl)-ethylamides and *N*-alkyl-erythronamides (104,105).

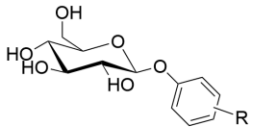

***O*-aryl-β-D-glucosides**
R = 4-Br, β-pBrPh-Glc;
% MGS 9.8 ± 0.82 % at 22 mM, IC_{50} 13.4 mM [95% CI = 11.1-16.0]

R = 4-OMe, β-PMP-Glc;
% MGS 22.9 ± 1.03 % at 22 mM, IC_{50} 28.8 mM [95% CI = 26.5-31.2]

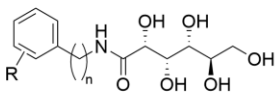

***N*-aryl-D-gluconamides**
n = 0, R = 2-F, 2FA;
% MGS 2.6 ± 0.37 % at 22 mM, IC_{50} 3.5 mM [95% CI = 3.41-3.52]

n = 1, R = 2,6-F, 2,6DFB;
% MGS 12.3 ± 0.74 % at 22 mM, IC_{50} 10.5 mM [95% CI = 8.69-12.7]

Figure 6. Structures and ice recrystallization inhibition activity of representative *O*-aryl-β-D-glucosides and *N*-aryl-D-gluconamides (67,101,108, 109, 110).

Furthermore, ice recrystallization inhibition activity increases with hydrophobic chain lengths from 5 to 14 carbons within the *N*-alkyl-2-(α-D-galactopyranosyl)-ethylamide class (Figure 5) (105). However, carbohydrates with a smaller hydrophilic component (e.g. the *N*-alkyl-erythronamides, Figure 5), have reduced activity compared to the corresponding *N*-alkyl-D-aldonamide with the same alkyl chain length (104).

Overall, these findings imply that a balance between the hydrophobic and hydrophilic components of a small-molecule IRI (amphiphilicity) is crucial to the activity optimization process. It is hypothesized that the hydrophobic component is required to disrupt the bulk water layer that ultimately results in ice recrystallization inhibition, while the hydrophilic component is required to maintain adequate solubility within the aqueous environment.

Despite the ability for these non-ionic surfactants to inhibit ice recrystallization, their use in biological systems as CPAs is limited. The highly hydrophobic alkyl chain can mediate membrane solubilization and can be cytotoxic (38, 106, 107). For example, addition of NOGlc as an additive for the cryopreservation of red blood cells (RBCs) resulted in significant post-thaw hemolysis (34 ± 1.0 % RBC integrity compared to 80 ± 4.5 % for the 20 % glycerol control) (38). In addition, compounds with a greater proportion of hydrophobicity suffer from dramatic reductions in aqueous solubility, thus limiting their use in biological applications as CPAs.

To overcome the issues arising from the physical properties of surfactant and hydrogelator IRIs, *O*-aryl-β-D-glucoside and *N*-aryl-D-gluconamide targets have been investigated (Figure 6). Substitution of the alkyl for an aryl functional group ensures a facile synthesis and reduces the risk of cytotoxicity associated with the long alkyl chain, while maintaining ice recrystallization inhibition activity. From these studies, several molecules are found to be effective inhibitors of ice recrystallization including (67, 108, 109, 110): 4-bromophenyl-β-D-glucose (β-*p*BrPh-Glc), 4-methoxyphenyl-β-D-glucose (β-PMP-Glc), *N*-(2-fluorophenyl-D-gluconamide (2FA), and *N*-(2,6-difluorobenzyl-D-gluconamide (2,6DFB) (Figure 6). Of note, 2FA exhibits greater ice recrystallization inhibition activity than any other small-molecule IRI reported to date while continuing to lack observable TH activity or DIS (101).

Overall, extensive SAR investigations have shown that small-molecule IRIs can exhibit ice recrystallization inhibition activity comparable to that observed in the presence of native AF(G)Ps. In addition, investigations into the mechanism of action of these compounds confirm that a balance between hydrophobicity and hydrophilicity is required to exhibit ice recrystallization inhibition activity while maintaining solubility in aqueous media.

Finally, these studies confirm that the activity of small-molecule IRIs can be modulated, optimized, and custom-tailored. However, further optimization of these hit compounds would be required to achieve improved potency and reduce the concentrations required for effective ice recrystallization inhibition. More importantly, while successful acellular assay data regarding the activity of these compounds is promising, it is imperative that the hit compounds are also tested in vitro for cytotoxicity and cryopreservation efficacy (cryo-efficacy).

CRYOPRESERVATION USING SMALL-MOLECULE IRIs

The complexity of the cellular system increases the difficulty of determining the biological effectiveness and/or applicability of a hit IRI. Therefore, guided by detailed SAR data on the acellular inhibition activity gathered by the SCA, cytotoxicity (in the absence of cryopreservation), and subsequent cryo-efficacy must also be tested. Baseline "end-point" cytotoxicity (18- to 24-hour compound exposure) is tested in relevant cell models for the desired cryopreservation application before it proceeds to cryopreservation experiments. As the cell's explicit exposure to CPAs during the cryopreservation process is significantly shorter than 18 hours, the "end-point" cytotoxicity measurement serves as a checkpoint for screening out compounds which, when considered alongside ice recrystallization inhibition activity, do not meet desired thresholds.

Furthermore, the sensitivity of a cell to the effects of cryopreservation can be directly correlated to its cellular complexity. For example, cryopreservation of RBCs has been possible since the 1950s (16), yet

cryopreservation of non-terminally differentiated cells such as mesenchymal stromal cells (MSCs) remains a significant challenge (33, 34, 35, 36, 37). While initial cryopreservation success may be observed immediately post-thaw, significant death and functionality loss of the MSCs is often observed within 24-48 hours due to triggered stress-induced biomolecular pathways (2, 111). Therefore, it is imperative that optimizing cryopreservation outcomes considers not only changes to post- thaw viability, but also cell recovery and downstream functionality for each individual cell type to ensure that the cryopreserved product resembles the unfrozen product as closely as possible.

Over the last several decades small-molecule IRIs have been shown to successfully improve the cryopreservation outcomes of a wide variety of cell types. While initial cryo-efficacy of the IRIs was often tested in RBC units due to their low cellular complexity, recent testing of IRIs with more complex cells, including several stem/progenitor cells has also been achieved. The success of these IRIs and their potential to dramatically improve the accessibility of cryopreserved biotherapeutics, as well as their clinical efficacy, will be discussed in the subsequent sections.

Cryopreservation of red blood cells

There is significant demand for viable, functional, and easily accessible RBC units. Therefore, the ability to effectively cryopreserve RBCs is essential to the field of transfusion medicine. Currently, the North American industry standard conditions for the cryopreservation of RBCs use glycerol as the CPA, which necessitates a time-consuming deglycerolization process prior to transfusion to prevent osmolysis (16, 39, 112). Therefore, cryopreserved RBC units are not routinely used in emergency transfusion medicine (112, 113). Lowering the required glycerol concentration (currently 40 %) by introducing alternative CPAs to the cryopreservation protocol can reduce deglycerolization times and facilitate improved patient treatments (114). A variety of CPA alternatives have been proposed that successfully eliminate the use of glycerol for RBC cryopreservation entirely, including salidroside and hydroxyethyl starch (115, 116). In addition, deglycerolization methods have been proposed to improve the time constraints that preclude the use of cryopreserved RBCs clinically (117). Alternatively, successful cryopreservation with significant improvement to cryopreservation outcomes can be achieved at reduced glycerol concentrations with the use of small-molecule IRIs (38).

Low concentrations of IRIs β-pBrPh-Glc and β-PMP-Glc in combination with only 15 % glycerol improve the post-thaw integrity of RBC membranes, a direct measure of RBC viability (118), compared to the industry standard using both slow and rapid cooling protocols (38, 119). For instance, when cells are slowly cooled (-1 °C/min) to –40 °C, the percentage of RBCs with intact membranes significantly increases ($p < 0.0001$) from 27.2 % (± 1.53) using only 15 % glycerol to 47.8 % (± 2.36) with the addition of 110 mM β-PMP-Glc and 68.9 % (± 1.82) with the addition of 30 mM β-pBrPh-Glc (Figure 7A) (38). Furthermore, 30 mM β-pBrPh-Glc in 15 % glycerol maintains RBC membrane integrity post-thaw comparable to the 40 % glycerol control following several cycles of transient warming events (120). These results demonstrate the value of inhibiting ice recrystallization under true cryopreservation storage conditions.

However, while reduced glycerol concentrations that maintain viable RBCs immediately post-thaw are achievable in the presence of small-molecule IRIs, the deglycerolization process remains problematic for some IRIs (121, 122). It has been hypothesized that interactions between β-pBrPh-Glc and the RBC membrane increases their susceptibility to the osmotic stress that occurs during deglycerolization (121). Recent investigations of RBCs frozen with a new IRI candidate 4-azidophenyl-β-D-glucose (β-pN_3Ph-Glc, 20 mM) and 15 % glycerol have comparable quality and function following cryopreservation, deglycerolization, and 4 °C storage to RBCs cryopreserved with 40 % glycerol alone at 24-hour and 7-day storage time points (121). Functional quality of RBCs is tested using several assays that monitor mean cell volume, ATP levels, 2,3-diphosphoglycerate concentration, methemoglobin concentration, oxygen affinity, membrane deformability, and extracellular potassium and sodium levels (118). These findings suggest that further optimization of the freezing, thawing, and deglycerolization conditions and additional IRI development could lead to successful cryopreservation of RBCs using small-molecule IRIs with dramatically reduced glycerol concentrations.

Cryopreservation of hematopoietic stem and progenitor cells from umbilical cord blood

Hematopoietic stem and progenitor cell (HSPC) products derived from umbilical cord blood (UCB) can be used as a life-saving treatment for several hematological, immune-deficiency, and metabolic disorders as well as for other novel therapies (14, 22, 123). Current cryopreservation protocols use a low concentration DMSO solution, yielding 70-80 % post-thaw viability (124, 125). However, delayed onset cell death and poor post-thaw cell quality result in reduced post-thaw engraftment and downstream clinical outcomes due to increased levels of apoptotic CD34+ cells and reduced proliferation and differentiation of the HSPCs (120, 126, 127, 128, 129, 130, 131, 132, 133). For example, UCB CD34+ cells that showed signs of apoptosis post-thaw failed to engraft when transplanted into immunodeficient mice (134). Therefore, improved cryopreservation protocols for HSPCs and UCB-derived cellular products are required.

The ability for IRIs to improve the cryopreservation of HSPCs was initially investigated using *N*-aryl-D-aldonamides including 2FA and 2,6-DFB (108). No significant increase in the percent post-thaw viability of CD34+ cells from the cryopreserved leukocyte concentrate of UCB is observed in the presence of either IRI when compared to the 10

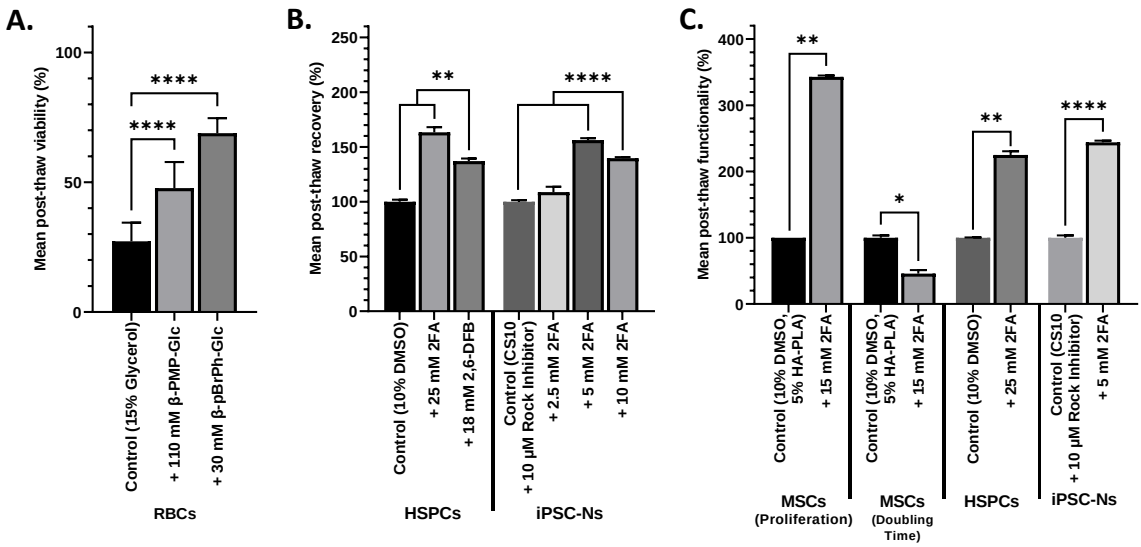

Figure 7. Comparison of cryopreservation outcomes in the presence of small-molecule IRIs compared to control cryopreservation solutions. **(A)** Post-thaw RBC integrity (viability). RBCs were cooled to -40 ºC and stored at −80 ºC prior to post-thaw hemolysis quantification by Drabkin's assay. 15 % glycerol alone (n = 22), 110 mM β-PMP-Glc (n = 18), 30 mM β-pBrPh-Glc (n = 10) (38). **(B)** Post-thaw recovery of HSPCs and iPSC-Ns normalized to their respective controls. Leukocyte concentrates containing CD34+ HSPCs and iPSC-Ns (derived from HMBEC-iPSCs) were cooled to -80 ºC and stored at -196 ºC prior to analysis of cell recovery by flow cytometry for HSPCs (n = 3) and Trypan blue exclusion assay for iPSC-Ns (n = 3) (108, 110). **(C)** Functionality testing of three different cell types following cryopreservation, normalized to their respective controls. MSCs were cryopreserved using an optimized step-down cooling procedure in a rate-controlled freezer to -180 ºC. Post-thaw functionality was assessed by Edu proliferation assay and cell counts (population doubling) and compared to the control solution (n = 2) (154). HSPCs were cryopreserved using the same method described in panel B. Post-thaw functionality was assessed using a long-term culture-initiating cell (LTC-IC) assay and compared to the control solution (n = 2) (108). iPSC-Ns were cryopreserved using the same method described in panel B. Functionality was assessed by recording electrical activity from the cells on microelectrode arrays (MEAs) after 236 days and compared to the control solution (n = 3) (110). All samples with IRI were prepared as the control solution plus IRI. All cells frozen via slow cooling (-1 ºC/min) and rapid thawing (37 ºC water bath). All data mean ± SEM (except MSCs panel C, mean ± SD). Asterisks indicate statistical significance relative to the control determined by two-tailed unpaired student's T-test where $p < 0.05$ (*), 0.01 (**), 0.001 (***) or 0.0001 (****).

% DMSO control (108). However, the net post-thaw recovery of viable CD34+ cells is 1.6-fold greater when 2FA ($p < 0.01$ at 25 mM) is added to the cryosolution, and 1.4-fold greater for 2,6-DFB ($p < 0.01$ at 18 mM), compared to DMSO alone (Figure 7B) (108). In addition, when added to 10 % DMSO, 12.5 and 25 mM 2FA result in a 2-fold increase in the number of committed progenitor cells compared to DMSO alone or compared to compounds that are not active IRIs (108).

The stringent long-term culture-initiating cell assay (LTC-IC), which measures the frequency of progenitors that can self-renew and differentiate, was used to measure the post-thaw functionality of HSPCs cryopreserved in the presence of IRIs (135). A 2-fold increase in the ability to self-renew and differentiate is observed in post-thaw leukocyte concentrates supplemented with 2FA (25 mM, $p < 0.01$) (Figure 7C) and the total number of LTC-ICs recovered is always greater in cryopreserved samples supplemented with IRIs (108). Furthermore, combination of 2FA and DMSO for the cryopreservation of cord blood units (CBUs) results in higher levels of human platelets, increased levels of human bone marrow chimerism, and an increased number of human colony-forming unit progenitors in the bone marrow upon transplant of CBUs compared to DMSO alone (136). The addition of 2FA has no significant cytotoxic effects, nor negative impact on the multilineage differentiation and self-renewal ability of the HSPCs (136). Collectively, these results show that IRIs improve the post-thaw engraftment potential and functionality of HSPCs derived from UCB as well as whole CBUs.

Cryopreservation of platelets

Platelet cryopreservation methods have been developed that increase the shelf-life of platelets from less than a week to up to two years using DMSO (137,138). However, the cryopreservation process can cause up to a 30 % reduction in total cell count and reduces functionality compared to unfrozen platelets (139, 140, 141, 142, 143). The use of 2FA has improved cryopreservation outcomes in other cell models and indicated its potential success for platelet cryopreservation. While some platelet quality and functionality parameters could be improved with the addition of 11 mM 2FA, most parameters remained comparable to the standard cryopreservation conditions (144). In addition, poly(vinyl) alcohol (PVA), an active polymer IRI, does not mitigate cryopreservation induced damage for platelets (145). Therefore, these results provide crucial information that ice recrystallization is not the most likely source of damage that is occurring during the cryopreservation of platelets. Finally, these results highlight the need for cell-specific cryopreservation protocols. Successful implementation of a CPA in one cell type does not necessarily indicate success in other similar cell types due to potential differences in cryoinjury mechanisms and post-thaw biological processes.

Cryopreservation of mesenchymal stem cells

MSCs are attractive for cell-based therapies due to their immunomodulatory and tissue repair properties (146, 147, 148, 149, 150, 151, 152). Typically, MSCs are cultured and pooled from multiple donors to ensure sufficient cells for treatment, however they lose therapeutic potency following long periods of in vitro expansion (33, 146). Therefore, the use of cryopreservation for storage and banking of MSCs to ensure continued, reliable, access to treatment doses is desirable (33). Current cryopreservation conditions for MSCs result in post-thaw recovery and viability percentages that are comparable to unfrozen MSCs (33, 34, 35, 36, 37). However, MSC functionality (particularly their immunomodulatory properties and multilineage differentiation ability) can be significantly impaired post-cryopreservation (33, 34, 35, 36, 37). Currently, cryopreserved MSCs must be cultured for several days prior to patient treatment following cryopreservation to ensure sufficient clinical efficacy.

It was hypothesized that the reduced functionality of MSCs following cryopreservation is due to damage induced by ice recrystallization, therefore β-pBrPh-Glc (30 mM, for its success in RBCs) and 2FA (15 mM, for its success in HSPCs) were investigated as CPAs for MSCs. In this study, standard cryopreservation conditions (34, 153) for MSCs (10 % DMSO, 5% human serum albumin in plasmalyte-A) were used. As anticipated, cells cryopreserved with either small-molecule IRI had high immediate post-thaw viability and recovery rates that were comparable to the control conditions (> 70 % for all conditions) (154). Cells that had been cryopreserved with the addition of 2FA (15 mM), thawed, and then cultured for three days had significantly greater

proliferation rates, lower doubling times, and more population doublings (23.6 ± 1.6 %, 27.4 ± 3.6 h, 2.71 ± 0.32, respectively) than the control freezing conditions (6.88 %, 59.7 ± 5.3 h, 1.22 ± 0.10, respectively) (Figure 7C) (154). β-pBrPh-Glc showed significantly greater delayed-onset cell death upon culture of the MSCs post-thaw compared to the control conditions (154).

It is hypothesized that the cell death observed in β-pBrPh-Glc-treated MSCs is a result of metabolic processing of the IRI, where β-pBrPh-Glc is presumably hydrolyzed at the *O*-glycosidic linkage between the aryl substitution and the carbohydrate moiety. This complication is avoided in RBC cryopreservation as these cells do not have the necessary metabolic machinery. In the initial "end-point" cytotoxicity screening of β-pBrPh-Glc in Hep G2 cells, significant cell death was observed at concentrations greater than 11 mM (122). However, the promising ice recrystallization inhibition activity of β-pBrPh-Glc warranted further cryo-efficacy testing. Ultimately, despite the decreased exposure times of the cells to the IRI during the cryopreservation process, *O*-aryl-glycoside IRIs may be limited to use in non-nucleated cells at this time. In addition, these studies highlight the importance of considering the entire pharmacokinetic profile of CPAs when optimizing lead compounds for use in biological applications.

Cryopreservation of induced pluripotent stem cells

The successful cryopreservation of induced pluripotent stem cells (iPSCs) is critical to their wide-scale use in areas including regenerative medicine, disease modelling, and drug discovery (155, 156). Current cryopreservation strategies for iPSCs use commercially available DMSO-based cryopreservation media such as mFreSR®, Stem Alpha Cryo3, or most commonly Cryostor® 10 (CS10) (157, 158). However, iPSCs are extremely vulnerable to cryopreservation and typically suffer from low post-thaw recovery, viability, and functionality using these conditions (159, 160). Following the significant improvements to post-thaw functionality of cryopreserved MSCs (including the absence of metabolically induced delayed-onset cell death) with the addition of 2FA, it was hypothesized that the *N*-aryl-D-gluconamide family of IRIs could be successfully applied to iPSCs.

In fact, the addition of 2FA (10 mM) for the cryopreservation of iPSCs shows significant improvements to post-thaw viability and recovery (71.5 %, 65.0 %) compared to the control (mFreSR®; 46.0 %, 47.6 %) (110). These results are consistent with post-thaw viability following 6-months of storage at -196 °C (84.0 % vs. 64.0% respectively) (110). 2FA (10 mM) is also able to reduce delayed-onset cell death for cryopreserved iPSCs as measured by Caspase 3/7 activity compared to mFreSR® alone ($p < 0.05$) (110).

Furthermore, 2FA is also found to be able to successfully improve the cryopreservation outcomes of terminally differentiated, post-mitotic iPSC-derived neurons (iPSC-Ns; differentiated from HBMEC-iPSCs). Compared to CS10, post-thaw viability of iPSC-Ns is not significantly different with the addition of 2FA (5 mM) (54.0% vs. 67.2 % respectively) (110). However, post-thaw recovery of iPSC-Ns frozen with 5 mM or 10 mM 2FA is 1.5-fold greater ($p < 0.0001$) than the control (CS10) (Figure 7B) and the cells retained expression of key neuronal markers with normal neuropharmacological responses (110). When the electrophysiological properties of the neurons were assessed using multielectrode arrays (MEAs), iPSC-Ns cryopreserved with 5 mM 2FA begin to re-establish synaptic function and neuronal network activity 21 days earlier than CS10 alone (27 days vs. 48 days) and had a significantly greater number of active electrodes after 236 days in culture ($p < 0.0001$) (Figure 7C) (110). Typically, iPSC-Ns require anywhere from 60-days to 6-months to reach maturity in culture, which poses a significant challenge to their timely delivery and use as clinical therapeutics (161, 162, 163). Therefore, the success of 2FA for improving the post-cryopreservation recovery and functionality of iPSC-Ns, as well as for cryopreserved iPSCs, represents a potential avenue for long-term storage of these complex cell types. This success could improve the accessibility, feasibility, and timeliness of cell-based therapies for a variety of diseases as well as critical iPSC-related research. Collectively, this data demonstrates that supplementing commercially available media formulations with IRIs represents a promising strategy for improved cryopreservation outcomes (recovery, functionality) of iPSCs and iPSC-Ns, which to date has been challenging to achieve. Future work must continue to explore the potential for IRIs to improve and optimize

the cryopreservation outcomes of other complex cell types that are sensitive to cryopreservation (cryo-sensitive).

THE FUTURE OUTLOOK OF SMALL-MOLECULE IRI-ASSISTED CRYOPRESERVATION

It is important to note that while several small-molecule IRIs have shown success in biological systems as highlighted in the previous section, no single uniform approach can be applied to all cell types. RBCs show improved outcomes using *O*-aryl-glycoside IRIs, yet these compounds show detrimental effects due to metabolically-induced cell death when used for the cryopreservation of MSCs. In addition, the *N*-aryl-D-gluconamide 2FA improves the post-thaw functionality of stem cell products (HSPCs, MSCs, iPSCs, and iPSC-Ns) compared to their respective controls, yet shows no improvement for the cryopreservation of platelets. More importantly, the metabolic stability and long-term biological effects of these small-molecule IRIs, as well as their effect on the entire cryopreservation chain, will be key to their successful large-scale deployment in cryopreservation applications.

Understanding of the mechanism of action of these small-molecule IRIs is critical for their continued optimization with specific cell types and cryopreservation conditions. Initial studies have shown that small-molecule ice recrystallization inhibition activity can be correlated to hydration number and that a balance between hydrophobicity and hydrophilicity is required (92, 93). Recently, SAR studies correlating ice recrystallization inhibition activity to other parameters such as the ratio of polar surface area to molecular surface area, octanol-water coefficient (logP), and other molecular features have not resulted in clear trends that can accurately predict activity (104). Additionally, while it is known that these IRIs do not bind to the ice surface (101, 122), exactly how each compound interacts with the bulk water layer between ice crystals to inhibit ice recrystallization is an extremely complex phenomenon that is not yet fully understood. This complexity adds to the difficulty of predicting which structural features of the small-molecule IRIs are essential to inhibit ice recrystallization and improve cryopreservation outcomes. Quantitative structure-activity relationship (QSAR)-assisted modeling of IRI candidates with respect to structural features can accurately predict whether a compound would be active (% MGS < 70 %) or inactive (% MGS > 70 %) at a success rate of 82 % (164). However, this model fails to discriminate between active IRIs more finely and thus is limited in its applicability for rational design. Therefore, while parameter-assisted predictions of SAR would dramatically improve the rational design of future IRIs, future research and further insight into a more detailed mechanism of action and the interactions between the IRIs and bulk water during cryopreservation is required.

It is also important to consider whether these small-molecule IRIs are capable of being internalized into a cell. Current CPAs that are capable of penetrating the cell membrane (e.g., DMSO and glycerol) help to maintain the osmotic pressure of cells undergoing cryopreservation (165). If small-molecule IRIs can be internalized into cells, it is possible that they could reduce the required concentration of DMSO and glycerol in cryopreservation media and help mitigate current CPA-induced toxicity by regulating cellular osmotic gradients. Studies of β-PMP-Glc and β-pBrPh-Glc in RBCs showed that their cryoprotective effect is consistent with the profile of a penetrating CPA (38, 119). In addition, these compounds are shown to inhibit ice recrystallization within the nucleus of cryopreserved HUVEC cells (119). Therefore, internalization of these small molecules into RBCs and other cell types can be inferred but has yet to be directly detected. Visualization of compound internalization using traditional tagging methods with large molecular weight fluorescent proteins must be avoided to prevent disruption of the natural cell environment. Raman microscopy imaging techniques provide an exciting avenue for the future study of small-molecule IRIs in the cellular environment.

Finally, previous studies have shown that a combination of small molecules can lead to improvements in cryopreservation outcomes. This improvement is hypothesized to be due to an additive effect where multiple avenues of cryoinjury are mitigated simultaneously and/or by resolving the pre-established limitations of one molecule through the addition of another (i.e., improvements to solubility, molecular stability, etc.) (32, 166, 167, 168). For instance, binary and ternary combinations of biocompatible molecules such as sugars and

poly-ols (i.e., D-glucose, D-trehalose, D-sucrose, or glycerol), amino acids (i.e., L-isoleucine or D-proline) and quaternary ammonium salts (i.e., choline chloride or betaine) have been shown to improve the cryopreservation outcomes of complex and cryo-sensitive cell types [such as iPSCs, HSCs, and adipose-derived stem cells (ADSCs)] beyond what was observed when cells were cryopreserved with the individual components (32, 166, 167, 168). As previously discussed, small-molecule IRIs have been shown to be most successful when glycerol or DMSO remained in the CPA solution. These results suggest that future work towards optimizing CPA mixtures containing combinations of IRIs that can target multiple mechanisms of cryoinjury could prove beneficial to the design of cell-specific cryopreservation strategies.

CONCLUSION

The development of small-molecule IRIs over the last several decades has resulted in dramatic improvements to the cryopreservation outcomes of several cell types. The development process includes the initial design and synthesis of candidate compounds, acellular screening of their ice recrystallization inhibition activity using a SCA, assessment of "end-point" cytotoxicity in a relevant cell model, followed by critical cryo-efficacy studies. The cryo-efficacy studies most importantly must focus on investigating all potential cryopreservation outcomes including the post-thaw viability, recovery, and functionality of the cells. Downstream clinical considerations must also be considered for IRI candidates including potential removal of the IRI, metabolic-induced effects, and long-term compound stability. As additional information is gathered on the mechanism of action of these small-molecule IRIs and the structural features required for their activity, additional emphasis must be placed on ensuring the biocompatibility and safety of the compounds for large-scale deployment in research, industrial, and clinical applications.

Notes: Authors L.E.M. and E.M.W. have no conflicts of interest to disclose. R.N.B is the chief scientific officer and co-founder of PanTHERA Cryosolutions Inc. (Ottawa, ON).

REFERENCES

1. Mazur P (1970) *Science* **168**, 939–949. 10.1126/science.168.3934.939.
2. Baust JG, Gao D & Baust JM (2009) *Organogenesis*, **5**(3), 90–96. 10.4161/org.5.3.10021.
3. Meneghel J, Kilbride P & Morris JG (2020) *Frontiers in Medicine* **7,** 10.3389/fmed.2020.592242.
4. Fuller BJ, Lane N & Benson EE (eds) (2004) *Life in the Frozen State*, 1st ed., CRC Press, Boca Raton, FL, 772 pp.
5. Gao D & Critser JK (2000) *ILAR Journal*, **41**(4), 187–196. 10.1093/ilar.41.4.187.
6. Mazur P (1984) *Am. J. Physiol. Cell Physiol.* **247**(3), C125–C142. 10.1152/ajpcell.1984.247.3.C125.
7. Fowler A & Toner M (2005) *Ann. N. Y. Acad. Sci.* **1066**(1), 119–135; 10.1196/annals.1363.010.
8. Gage AA & Baust J (1998) *Cryobiology*, **37**(3), 171–186. 10.1006/cryo.1998.2115.
9. Baust JM (2002) *Cell Preserv. Technol.* **1**(1), 17–31. 10.1089/15383440260073266.
10. Hubel A (2011) *Transfusion* **51**(s4), 82S-86S. 10.1111/j.1537-2995.2011.03370.x.
11. Whaley D Damyar K, Witek RP et al. (2021) *Cell Transplantation* **30,** 10.1177/0963689721999617.
12. Mazur P, Leibo SP & Chu EHY (1972) *Exp. Cell Res.* **71**(2), 345–355. 10.1016/0014-4827(72)90303-5.
13. Pegg DE (2007) in *Cryopreservation and Freeze-Drying Protocols*, *Methods in Molecular Biology*, (eds) Day JG & Stacey GN, Humana Press, Totowa, NJ, Vol. **368**, pp. 39–57. 10.1007/978-1-59745-362-2_3.
14. Hunt CJ (2011) *Transfus. Med. Hemotherapy* **38**(2), 107–123. 10.1159/000326623.
15. Polge C, Smith AU & Parkes AS (1949) *Nature* **164**, 666. 10.1038/164666a0.
16. Smith A (1950) *The Lancet* **256**(6644), 910–911. 10.1016/S0140-6736(50)91861-7.
17. Kojayan GG, Alexander M, Imagawa DK et al. (2018) *Islets* **10**(1), 40–49. 10.1080/19382014.2017.1405202.
18. Chen C (1986) *The Lancet* **327**(8486), 884–886. 10.1016/S0140-6736(86)90989-X.
19. Anger JT, Gilbert BR & Goldstein M (2003) *Journal of Urology* **170**(4.1), 1079–1084. 10.1097/01.ju.0000084820.98430.b8.

20. Berz D, McCormack EM, Winer ES et al. (2007) *Am. J. Hematol.* **82**(6), 463–472. 10.1002/ajh.20707.
21. Bahsoun S, Coopman K & Akam EC (2019) *J. Transl. Med.* **17**(1), 397. 10.1186/s12967-019-02136-7.
22. Iafolla MAJ, Tay J & Allan DS (2014) *Biol. Blood Marrow Transplant.* **20**(1), 20–25. 10.1016/j.bbmt.2013.09.010.
23. National Marrow Donor Program (Be the Match) (2022) *Updates for Transplant Centers and Cooperative Registries - Up-to-date information on NMDP/Be The Match response to COVID-19* https://network.bethematchclinical.org/news/nmdp/be-the-match-response-to-covid-19/updates-for-transplant-centers-and-cooperative-registries/#Cryopreservation (accessed Oct 27, 2022).
24. Passweg JR, Baldomero H, Chabannon C. et al. (2020) *Bone Marrow Transplantation*, **55**(8), 1604–1613. 10.1038/s41409-020-0826-4.
25. Lovelock JE & Bishop MWH (1959) *Nature* **183**(4672), 1394–1395. 10.1038/1831394a0.
26. Awan M, Buriak I, Fleck R et al. (2020) *Regenerative Medicine* **15**(3), 1463–1491. 10.2217/rme-2019-0145.
27. Brayton CF (1986) *The Cornell Veterinarian* **76**(1), 61–90.
28. David NA (1972) *Annu. Rev. Pharmacol.* **12**(1), 353–374. 10.1146/annurev.pa.12.040172.002033.
29. Shu Z, Heimfeld S & Gao D (2014) *Bone Marrow Transplantation* **49**(4), 469–476. 10.1038/bmt.2013.152.
30. Ruiz-Delgado GJ, Mancías-Guerra C, Tamez-Gómez EL et al. (2009) *Acta Haematologica* **122**(1), 1–5. 10.1159/000227267.
31. Motta JPR, Paraguassú-Braga FH, Bouzas LF et al. (2014) *Cryobiology* **68**(3), 343–348. 10.1016/j.cryobiol.2014.04.007.
32. Rodrigues JP, Paraguassú-Braga FH, Carvalho L et al. (2008) *Cryobiology* **56**(2), 144–151. 10.1016/j.cryobiol.2008.01.003.
33. Yong KW, Wan Safwani WKZ, Xu F et al. (2015) *Biopreserv. Biobanking* **13**(4), 231–239. 10.1089/bio.2014.0104.
34. Pollock K, Sumstad D, Kadidlo D et al. (2015) *Cytotherapy* **17**(1), 38–45. 10.1016/j.jcyt.2014.06.008.
35. Marquez-Curtis LA, Janowska-Wieczorek A, McGann LE et al. (2015) *Cryobiology* **71**(2), 181–197, 10.1016/j.cryobiol.2015.07.003.
36. François M, Copland IB, Yuan S et al. (2012) *Cytotherapy* **14**(2), 147–152. 10.3109/14653249.2011.623691.
37. Moll G, Alm JJ, Davies LC et al. (2014) *Stem Cells* **32**(9), 2430–2442. 10.1002/stem.1729.
38. Capicciotti CJ, Kurach JDR, Turner TR et al. (2015) *Scientific Reports* **5**(1), 9692. 10.1038/srep09692.
39. Meryman HT & Hornblower M (1972) *Transfusion* **12**(3), 145–156. 10.1111/j.1537-2995.1972.tb00001.x.
40. Gurtovenko, A.A. and Anwar, J. (2007) *J. Phys. Chem. B*, **111**(35), 10453–10460. 10.1021/jp073113e.
41. Notman R, Noro M, O'Malley B et al. (2006) *J. Am. Chem. Soc.* **128**(43), 13982–13983. 10.1021/ja063363t.
42. Gordon MS, Amdur BH & Scholander PF (1962) *The Biological Bulletin* **122**(1), 52–62. 10.2307/1539321.
43. Scholander PF, van Dam L, Kanwisher JW et al. (1957) *J. Cell. Comp. Physiol.* **49**(1), 5–24. 10.1002/jcp.1030490103.
44. Devries AL (1982) *Comp. Biochem. Physiol., Part A: Mol. Integr. Physiol.*, **73**(4), 627–640. 10.1016/0300-9629(82)90270-5.
45. Capicciotti CJ, Doshi M & Ben RN (2013) in *Recent Developments in the Study of Recrystallization*, (ed) Wilson P, InTech, pp. 177–224. 10.5772/54992.
46. Duman JG & DeVries AL (1974) *Nature* **247**(5438), 237–238. 10.1038/247237a0.
47. Wilson PW (1993) *CryoLetters* **14**, 31–36.
48. Knight CA & DeVries AL (1994) *J. Cryst. Growth* **143**(3-4), 301–310. 10.1016/0022-0248(94)90071-X.
49. Raymond JA & DeVries AL (1977) *Proc. Natl. Acad. Sci. U.S.A.* **74**(6), 2589–2593. 10.1073/pnas.74.6.2589.
50. Knight CA, DeVries AL & Oolman LD (1984) *Nature* **308**(5956), 295–296. 10.1038/308295a0.
51. Knight CA, Driggers E & DeVries AL (1993) *Biophysical Journal* **64**(1), 252–259. 10.1016/S0006-3495(93)81361-4.
52. Knight CA, Cheng CC & DeVries AL (1991) *Biophysical Journal* **59**(2), 409–418. 10.1016/S0006-3495(91)82234-2.
53. Kristiansen E & Zachariassen KE (2005) *Cryobiology* **51**(3), 262–280. 10.1016/j.cryobiol.2005.07.007.

54. Budke C & Koop T (2020) in *Antifreeze Proteins, Volume 2*, (eds) Ramlov H & Friis D, Springer, Cham, Switzerland.
55. Urbańczyk M, Góra J, Latajka R et al. (2017) *Amino Acids* **49**(2), 209–222. 10.1007/s00726-016-2368-z.
56. Christner BC (2010) *Appl. Microbiol. Biotechnol.* **85**(3), 481–489. 10.1007/s00253-009-2291-2.
57. Tab MM, Hashim NHF, Najimudin N et al. (2018) *Arabian J. Sci. Eng.* **43**(1), 133–141. 10.1007/s13369-017-2738-1.
58. Venketesh S & Dayananda C (2008) *Crit. Rev. Biotechnol.* **28**(1), 57–82. 10.1080/07388550801891152.
59. Solomon RG & Appels R (1999) *Protein Expression and Purification* **16**(1), 53–62. 10.1006/prep.1999.1040.
60. Tomczak MM, Marshall CB, Gilbert JA et al. (2003) *Biochem. Biophys. Res. Commun.* **311**(4), 1041–1046. 10.1016/j.bbrc.2003.10.106.
61. Smallwood M, Worrall D, Byass L et al. (1999) *The Biochemical Journal* **340**(2), 385–391.
62. Mitchell DE, Congdon T, Rodger A et al. (2015) *Scientific Reports* **5**(1), 15716. 10.1038/srep15716.
63. Graham LA, Agrawal P, Oleschuk RD et al. (2018) *Cryobiology* **81**, 138–144. 10.1016/j.cryobiol.2018.01.011.
64. Knight CA, Hallett J & DeVries AL (1988) *Cryobiology* **25**, 55–60. 10.1016/0011-2240(88)90020-X.
65. Horwath KL, Easton CM, Poggioli GJ et al. (1996) *Eur. J. Entomol.* **93**(3), 419–433.
66. Jackman J, Noestheden M, Moffat D et al. (2007) *Biochem. Biophys. Res. Commun.* **354**(2), 340–344. 10.1016/j.bbrc.2006.12.225.
67. Abraham S, Keillor K, Capicciotti CJ et al. (2015) *Cryst. Growth Des.* **15**(10), 5034–5039; 10.1021/acs.cgd.5b00995.
68. Ampaw AA, Sibthorpe A & Ben RN (2021) in *Cryopreservation and Freeze-Drying Protocols*, *Methods in Molecular Biology*, (eds) Wolkers WF & Oldenhof H, **Vol. 2180.** Springer US, New York, NY, pp. 271–283. 10.1007/978-1-0716-0783-1_9.
69. Budke C, Dreyer A, Jaeger J et al. (2014) *Cryst. Growth Des.* **14**(9), 4285–4294. 10.1021/cg5003308.
70. Balcerzak AK, Capicciotti CJ, Briard JG et al. (2014) *RSC Adv.* **4**(80), 42682–42696. 10.1039/C4RA06893A.
71. Schneider CA, Rasband WS & Eliceiri KW (2012) *Nature Methods* **9**(7), 671–675. 10.1038/nmeth.2089.
72. Abraham S (2015) *Development and Implementation of a Kinetic Quantitative Analysis of Novel Small Molecule Ice Recrystallization Inhibitors*, MSc Thesis, University of Ottawa, Ottawa, ON. 10.20381/ruor-4055.
73. Olijve LLC, Oude Vrielink AS & Voets IK (2016) *Cryst. Growth Des.* **16**(8), 4190–4195. 10.1021/acs.cgd.5b01637.
74. Saad J, Fomich M, Día VP et al. (2023) *Cryobiology* **111**, 1–8. 10.1016/j.cryobiol.2023.02.002.
75. Tymkovych M, Gryshkov O, Selivanova K et al. (2021) in *8th European Medical and Biological Engineering Conference*, (eds) Jarm T, Cvetkoska A, Mahnič-Kalamiza S et al., *IFMBE Proceedings*, **Vol. 80.** Springer, Cham, Switzerland, 10.1007/978-3-030-64610-3_13.
76. Komatsu S, DeVries AL & Feeney RE (1970) *The Journal of Biological Chemistry* **245**(11), 2909–2913. 10.1016/S0021-9258(18)63074-1.
77. Ahmed AI, Osuga DT & Feeney RE (1973) *Journal of Biological Chemistry* **248**(24), 8524–8527. 10.1016/S0021-9258(19)43164-5.
78. Schrag JD & DeVries AL (1983) *Comp. Biochem. Physiol., Part A: Mol. Integr. Physiol.* **74**(2), 381–385. 10.1016/0300-9629(83)90619-9.
79. Tachibana Y, Fletcher GL, Fujitani N et al. (2004) *Angew. Chem., Int. Ed.*, **43**(7), 856–862. 10.1002/anie.200353110.
80. Peltier R, Brimble MA, Wojnar JM et al. (2010) *Chem. Sci.* **1**, 538–551. 10.1039/c0sc00194e.
81. Yeh Y & Feeney RE (1996) *Chem. Rev.* **96**(2), 601–618. 10.1021/cr950260c.
82. Harding MM, Ward LG & Haymet ADJ (1999) *European Journal of Biochemistry* **264**(3), 653–665. 10.1046/j.1432-1327.1999.00617.x.
83. William N, Mangan S, Ben RN et al. (2023) *Annu. Rev. Biomed. Eng.* **25**(1), 333–362. 10.1146/annurev-bioeng-082222-015243.
84. Liu S & Ben RN (2005) *Org. Lett.* **7**(12), 2385–2388; 10.1021/ol050677x.
85. Eniade A, Purushotham M, Ben RN et al. (2003) *Cell Biochem. Biophys.* **38**(2), 115–124. 10.1385/CBB:38:2:115.

86. Ravishankar R, Surolia A, Vijayan M et al. (1998) *J. Am. Chem. Soc.* **120**(44), 11297–11303. 10.1021/ja982193k.
87. Leclère M, Kwok BK, Wu LK et al. (2011) *Bioconjugate Chemistry* **22**(9), 1804–1810. 10.1021/bc2001837.
88. Li T, Zhao Y, Zhong Q et al. (2019) *Biomacromolecules* **20**(4), 1667–1674. 10.1021/acs.biomac.9b00027.
89. Biggs CI, Bailey TL, Ben Graham et al. (2017) *Nature Communications* **8**(1), 1546. 10.1038/s41467-017-01421-7.
90. Budke C & Koop T (2006) *ChemPhysChem* **7**(12), 2601–2606. 10.1002/cphc.200600533.
91. Tachibana Y, Matsubara N, Nakajima F et al. (2002) *Tetrahedron* **58**(51), 10213–10224; 10.1016/S0040-4020(02)01359-5.
92. Czechura P, Tam RY, Dimitrijevic E et al. (2008) *J. Am. Chem. Soc.* **130**(10), 2928–2929. 10.1021/ja7103262.
93. Tam RY, Ferreira SS, Czechura P et al. (2008) *J. Am. Chem. Soc.* **130**(51), 17494–17501. 10.1021/ja806284x.
94. van der Wal S, Capicciotti CJ, Rontogianni S et al. (2014) *MedChemComm* **5**(8), 1159–1165. 10.1039/C4MD00013G.
95. Budke C, Heggemann C, Koch M et al. (2009) *J. Phys. Chem. B* **113**(9), 2865–2873. 10.1021/jp805726e.
96. Sutton RL, Lips A, Piccirillo G et al. (1996) *J. Food Sci.* **61**(4), 741–745. 10.1111/j.1365-2621.1996.tb12194.x.
97. Hagiwara T, Hartel RW & Matsukawa S (2006) *Food Biophysics* **1**(2), 74–82. 10.1007/s11483-006-9009-0.
98. Alley RB, Perepezko JH & Bentley CR (1986) *Journal of Glaciology* **32**(112), 415–424. 10.3189/S0022143000012120.
99. Knight CA (1966) *Journal of Applied Physics* **37**(2), 568–574. 10.1063/1.1708217.
100. Gleiter H (1969) *Acta Metallurgica* **17**(5), 565–573. 10.1016/0001-6160(69)90115-1.
101. McMunn LE, D'Costa AS, Bordenave N et al. (2023) *J. Phys. Chem. Lett.* **14**(26), 6043–6050. 10.1021/acs.jpclett.3c00845.
102. Galema SA & Hoeiland H (1991) *J. Phys. Chem.* **95**(13), 5321–5326. 10.1021/j100166a073.
103. Capicciotti CJ, Leclère M, Perras FA et al. (2012) *Chem. Sci.* **3**(5), 1408–1416. 10.1039/c2sc00885h.
104. Ampaw A, Charlton TA, Briard JG et al. (2019) *Peptide Science* **111**(1), e24086. 10.1002/pep2.24086.
105. Trant JF, Biggs RA, Capicciotti CJ et al. (2013) *RSC Advances* **3**(48), 26005–26009. 10.1039/c3ra43835j.
106. Baron C & Thompson TE (1975) *Biochim Biophys Acta Biomembr.* **382**(3), 276–285. 10.1016/0005-2736(75)90270-9.
107. Hildreth JEK (1982) *Biochemical Journal* **207**(2), 363–366. 10.1042/bj2070363.
108. Briard JG, Jahan S, Chandran P et al. (2016) *ACS Omega* **1**(5), 1010–1018. 10.1021/acsomega.6b00178.
109. Capicciotti CJ, Mancini RS, Turner TR et al. (2016) *ACS Omega* **1**(4), 656–662. 10.1021/acsomega.6b00163.
110. Alasmar S, Huang J, Chopra K et al. (2023) *Stem Cells* **41**(11), 1006-1021. 10.1093/stmcls/sxad059.
111. Baust JM, Vogel MJ, Van Buskirk R et al. (2001) *Cell Transplantation* **10**(7), 561–571.
112. Scott KL, Lecak J & Acker JP (2005) *Transfus. Med. Rev.* **19**(2), 127–142. 10.1016/j.tmrv.2004.11.004.
113. Hess JR (2004) *Transfusion Medicine* **14**(1), 1–8. 10.1111/j.0958-7578.2004.00472.x.
114. Miloš Bohoněk (2012) in *Blood Transfusion in Clinical Practice*, (ed) Kochhar P, INTECH Open Access Publisher, pp. 233–242. 10.5772/36146.
115. Alotaibi NAS, Slater NKH & Rahmoune H (2016) *PLOS ONE* **11**(9), e0162748. 10.1371/journal.pone.0162748.
116. Sputtek A, Kühnl P & Rowe AW (2007) *Transfus Med Hemother* **34**(4), 262–267. 10.1159/000104136.
117. Lelkens CCM, de Korte D & Lagerberg JWM (2015) *Vox Sanguinis* **108**(3), 219–225. 10.1111/vox.12219.
118. Orlov D & Karkouti K (2015) *Anaesthesia* **70**, 29-e12. 10.1111/anae.12891.
119. Poisson JS, Acker JP, Briard JG et al. (2019) *Langmuir* **35**(23), 7452–7458. 10.1021/acs.langmuir.8b02126.
120. Briard JG, Poisson JS, Turner TR et al. (2016) *Sci. Rep.* **6**(1), 23619. 10.1038/srep23619.
121. Poisson J (2019) *Synthesis and In Vitro Applications of Ice Recrystallization Inhibitors*, PhD Thesis, University of Ottawa, Ottawa, ON. http://hdl.handle.net/10393/39466.

122. Capicciotti C (2014) *The Rational Design of Potent Ice Recrystallization Inhibitors for Use as Novel Cryoprotectants*, PhD Thesis, University of Ottawa, Ottawa, ON. 10.20381/ruor-3544.
123. Harris DT (2009) *British Journal of Haematology* **147**(2), 177–184. 10.1111/j.1365-2141.2009.07767.x.
124. Rubinstein P, Dobrila L, Rosenfield RE et al. (1995) *Proc. Natl. Acad. Sci. U.S.A.* **92**(22), 10119–10122. 10.1073/pnas.92.22.10119.
125. Hornberger K, Yu G, McKenna D et al. (2019) *Transfus Med Hemother* **46**(3), 188–196. 10.1159/000496068.
126. Allan D, Keeney M, Howson-Jan K et al. (2002) *Bone Marrow Transplantation* **29**(12), 967–972. 10.1038/sj.bmt.1703575.
127. Abrahamsen JF, Wentzel-Larsen T & Bruserud Ø (2004) *Cytotherapy* **6**(4), 356–362. 10.1080/14653240410004925.
128. Donaldson C, Armitage WJ, Denning-Kendall PA et al. (1996) *Bone Marrow Transplantation* **18**(4), 725–731.
129. Gao DY, Chang Q, Liu C et al. (1998) *Cryobiology* **36**, 40–48. 10.1006/cryo.1997.2060.
130. Yang H, Acker JP, Cabuhat M et al. (2005) *Bone Marrow Transplantation* **35**(9), 881–887. 10.1038/sj.bmt.1704926.
131. Wu L, Al-Hejazi A, Filion L et al. (2012) *Cytotherapy* **14**(2), 205–214. 10.3109/14653249.2011.610302.
132. Sasnoor LM, Kale VP & Limaye LS (2003) *J. Hematother. Stem Cell Res.* **12**(5), 553–564. 10.1089/152581603322448268.
133. Sasnoor LM, Kale VP & Limaye LS (2005) *Transplantation* **80**(9), 1251– 1260. 10.1097/01.tp.0000169028.01327.90.
134. Shim J-S, Cho B, Kim M et al. (2006) *Br. J. Haematol.* **135**(2), 210–213. 10.1111/j.1365-2141.2006.06270.x.
135. Coulombel L (2004) *Oncogene* **23**(43), 7210–7222. 10.1038/sj.onc.1207941.
136. Jahan S, Adam MK, Manesia JK et al. (2020) *Transfusion* **60**(4), 769–778. 10.1111/trf.15759.
137. Noorman F, van Dongen TTCF, Plat M-CJ et al. (2016) *PLOS ONE* **11**(12), e0168401. 10.1371/journal.pone.0168401.
138. Valeri CR, Ragno G & Khuri S (2005) *Transfusion* **45**(12), 1890–1898. 10.1111/j.1537-2995.2005.00647.x.
139. Johnson L, Coorey CP & Marks DC (2014) *Transfusion* **54**(8), 1917–1926. 10.1111/trf.12578.
140. Dumont LJ, Cancelas JA, Dumont DF et al. (2013) *Transfusion* **53**(1), 128–137. 10.1111/j.1537-2995.2012.03735.x.
141. Crimmins D, Flanagan P, Charlewood R et al. (2016) *Transfusion* **56**(11), 2799–2807. 10.1111/trf.13763.
142. Waters L, Padula MP, Marks DC et al. (2017) *Transfusion* **57**(12), 2845–2857. 10.1111/trf.14310.
143. Raynel S, Padula MP, Marks DC et al. (2015) *Transfusion* **55**(10), 2422–2432. 10.1111/trf.13165.
144. Waters L, Ben R, Acker JP et al. (2020) *Cryobiology* **96**, 152–158. 10.1016/j.cryobiol.2020.07.003.
145. Six KR, Lyssens S, Devloo R et al. (2019) *Transfusion* **59**(9), 3029–3031. 10.1111/trf.15395.
146. Ullah I, Subbarao RB & Rho GJ (2015) *Bioscience Reports* **35**(2), e00191.10.1042/BSR20150025.
147. Bashir J, Sherman A, Lee H et al. (2014) *PM&R* **6**(1), 61–69. 10.1016/j.pmrj.2013.05.007.
148. Freitag J, Bates D, Boyd R et al. (2016) *BMC Musculoskeletal Disorders* **17**(1), 230. 10.1186/s12891-016-1085-9.
149. Thakker R & Yang P (2014) *Curr. Treat. Options Cardiovasc. Med.* **16**(7), 323. 10.1007/s11936-014-0323-4.
150. Kalinina NI, Sysoeva VY, Rubina KA et al. (2011) *Acta Naturae* **3**(4), 30–37. 10.3389/fimmu.2013.00201.
151. Lavorato A, Raimondo S, Boido M et al. (2021) *International Journal of Molecular Sciences* **22**(2), 572. 10.3390/ijms22020572.
152. Margiana R, Markov A, Zekiy AO et al. (2022) *Stem Cell Research & Therapy* **13**(1), 366. 10.1186/s13287-022-03054-0.
153. Vemuri M, Chase LG & Rao MS (eds.) (2011) *Mesenchymal Stem Cell Assays and Applications*; *Methods in Molecular Biology* **Vol. 698**, Humana Press, Totowa, NJ. 10.1007/978-1-60761-999-4.
154. Khan S, Poisson J, Davila L et al. (2019) *Cytotherapy* **21**(5), S76. 10.1016/j.jcyt.2019.03.477.
155. Singh VK, Kalsan M, Kumar N et al. (2015) *Front. Cell Dev. Biol.* **3**(2), 10.3389/fcell.2015.00002.

156. Wu SM & Hochedlinger K (2011) *Nature Cell Biology* **13**(5), 497–505. 10.1038/ncb0511-497.
157. Lam RS, Töpfer FM, Wood PG et al. (2017) *PLoS ONE* **12**(1), e0169506. 10.1371/journal.pone.0169506.
158. Gavin-Plagne L, Perold F, Osteil P et al. (2020) *Int. J. Mol. Sci.* **21**(19), 7285. 10.3390/ijms21197285.
159. Nishiyama Y, Iwanami A, Kohyama J et al. (2016) *Neuroscience Research* **107**, 20–29. 10.1016/j.neures.2015.11.011.
160. Imaizumi K, Nishishita N, Muramatsu M et al. (2014) *PLoS ONE* **9**(2), e88696. 10.1371/journal.pone.0088696.
161. Prè D, Nestor MW, Sproul AA et al. (2014) *PLoS ONE* **9**(7), e103418. 10.1371/journal.pone.0103418.
162. Huang C-Y, Liu C-L, Ting C-Y et al. (2019) *Journal of Biomedical Science* **26**(1), 87. 10.1186/s12929-019-0578-x.
163. Jezierski A, Baumann E, Aylsworth A et al. (2022) *Stem Cell Reviews and Reports* **18**(1), 259–277. 10.1007/s12015-021-10263-2.
164. Briard JG, Fernandez M, De Luna P et al. (2016) *Sci. Rep.* **6**(1), 26403. 10.1038/srep26403.
165. McGann LE (1978) *Cryobiology* **15**, 382–390. 10.1016/0011-2240(78)90056-1.
166. Li R, Hornberger K, Dutton JR et al. (2020) *Front. Bioeng. Biotechnol.* **8,** 10.3389/fbioe.2020.00001.
167. Jesus AR, Meneses L, Duarte ARC et al. (2021) *Cryobiology* **101**, 95–104. 10.1016/j.cryobiol.2021.05.002.
168. Zhang T-Y, Tan P-C, Xie Y et al. (2020) *Stem Cell Res Ther* **11**(1), 460. 10.1186/s13287-020-01969-0.